 doi:10.20944/preprints201709.0158.v1

Variational mode decomposition denoising combined with the Euclidean distance for diesel engine vibration signal

Gang Ren [1], Jide Jia [2] , Xiangyu Jia [1] , Jiajia Han [1]

[1] Postgraduate Training Brigade，Army Military Transportation University, Tianjin 300161, China; jjxyrengang@163.com (G.R.); lkittyyoyo_jxy@126.com (X.J.)

[2] Military Vehicle Department, Army Military Transportation University, Tianjin 300161, China; jide@ustc.edu (G.R.)

* Correspondence: jjxyrengang@163.com or jide@ustc.edu ; Tel:+86-022-84658841

Abstract: Variational mode decomposition (VMD) is a recently introduced adaptive signal decomposition algorithm with a solid theoretical foundation and good noise robustness compared with empirical mode decomposition (EMD). There is a lot of background noise in the vibration signal of diesel engine. To solve the problem, a denoising algorithm based on VMD and Euclidean Distance is proposed. Firstly, a multi-component, non-Gauss, and noisy simulation signal is established, and decomposed into a given number K of band-limited intrinsic mode functions by VMD. Then the Euclidean distance between the probability density function of each mode and that of the simulation signal are calculated. The signal is reconstructed using the relevant modes, which are selected on the basis of noticeable similarities between the probability density function of the simulation signal and that of each mode. Finally, the vibration signals of diesel engine connecting rod bearing faults are analyzed by the proposed method. The results show that compared with other denoising algorithms, the proposed method has better denoising effect, and the fault characteristics of vibration signals of diesel engine connecting rod bearings can be effectively enhanced.

Keywords: variational mode decomposition; Euclidean Distance; diesel engine; vibration signal; denoising algorithm

1. Introduction

Vibration signal processing has been an effective way of monitoring mechanical equipment for many years. However, mechanical vibration signal are usually masked by significant background noise, which have motivated many studies into developing denoising methods [1]. The vibration signals should be processed to reduce noise and improve the quality before further analyzing [2]. Many researchers in this field have made thorough explorations. Wavelet denoising is a very effective denoising method in recent years, among which wavelet threshold denoising is the most commonly used method [3-6]. However, the denoising effect of this method is affected by the selection of basis functions and depends on the subjective experience of the designer, which has uncertainty.

In order to solve the above problems, Huang et al. introduced an adaptive signal processing technique called empirical mode decomposition (EMD)[7,8], which has demonstrated outstanding

Preprints (www.preprints.org) | NOT PEER-REVIEWED | Posted: 29 September 2017 doi:10.20944/preprints201709.0158.v1

performance in dealing with nonlinear and nonstationary signals. This technique has been applied in many fields, such as biomedical image analysis [9], fault diagnosis of rolling element bearings [10], signal de-noising [11-13], and voice signal analysis [14]. According to the principle of wavelet threshold denoising, EMD threshold denoising is put forward [15,16]. In addition, EMD denoising combined with the Euclidean distance(ED) is proposed in document [17]. All these methods have achieved good denoising effect. However, EMD still has some disadvantages, such as mode mixing and the lack of an exact mathematical model of the process.

In recent years, Konstantin, Dragomiretskiy et al. proposed variational modal decomposition [18], which is essentially composed of several adaptive Wiener filters and has good noise robustness. Compared with EMD, VMD has strong mathematical theory basis. So it can effectively alleviate or avoid a series of problems that exist in EMD, and has higher operation efficiency. VMD is widely used in various engineering fields [19-22]. An X.L. et al. applied VMD to the bearing fault diagnosis of the wind turbine, and realized the effective discrimination of the bearing fault [23]. By combining VMD with detrended fluctuation analysis (DFA), Liu et al. successfully extracted gear fault characteristics [24]. By combining VMD with independent component analysis (ICA), Yao et al. successfully separated the piston knock and combustion noise of the engine [25]. Zhang M. et al proposed a denoising method based on VMD and correlation coefficient (VMD-CORR)[26]. However, because of the large amount of noise in the signal, it is easy to remove the useful components in the signal, which leads to the distortion of the signal.

In this paper, a denoising algorithm, called the VMD-Euclidean distance (VMD-ED), is presented for vibration signal of diesel engine. Firstly, a multi-component, non-stationary and non-Gauss simulation signal is established, and the Gauss white noise is added. Secondly, the simulation signal is decomposed by VMD to obtain the band limited intrinsic mode functions (BLIMFs). Then the probability density functions (PDF) of the simulation signal and each BLIMF are calculated respectively, and the ED between the PDF of the simulation signal and that of each BLIMF is calculated. A smaller ED value means that more features are contained in the signal under comparison; the relevant modes are thus selected to reconstruct the signal. To validate the denosing effect of the proposed scheme, several denosing methods are compared with VMD-ED under different evaluation criteria, including the root mean square error (RMSE), mean absolute error (MAE), and the output signal-to-noise ratio (SNR out). Compared with the denoising methods of document [17,26], the method proposed in this paper has better denoising effect. Finally, the noise of the fault signals of diesel engine connecting rod bearings is effectively eliminated by using VMD-ED, and the fault characteristic is highlighted.

2. Variational Mode Decomposition

The VMD algorithm defines the intrinsic mode function as a non-stationary AM-FM signal. The intrinsic mode is considered as follows:

$$u_k(t) = A_k(t)\cos(\varphi_k(t)) \tag{1}$$

Where the phase $\varphi_k(t)$ shall satisfy the following condition: $\varphi_k(t)' \geq 0$; the envelope line $A_k(t)$ should satisfy the following condition: $A_k(t) \geq 0$; the instantaneous frequency $\omega_k(t)$ should satisfy the following condition: $\omega_k(t) = \varphi_k(t)'$. $A_k(t)$ and $\omega_k(t)$ change slowly, and

Preprints (www.preprints.org) | NOT PEER-REVIEWED | Posted: 29 September 2017 doi:10.20944/preprints201709.0158.v1

$\varphi_k(t)$ changes more rapidly.

The Hilbert transform is performed for each modal function $u_k(t)$, and exponential correction is applied to obtain K modal functions. Then the frequency spectrum of the modal function is corrected to the estimated central frequency, and the bandwidth of the modal component is calculated by using Gauss smoothing. The variational constraint problem can be defined as follows:

$$\min_{\{u_k\},\{w_k\}}\{\sum_{k=1}^{K}\left\|a_t\{[(\delta(t)+\frac{j}{\pi t}]*u_k(t)\}e^{-j\omega_k t}\right\|_2^2\}\ s.t.\sum_{k=1}^{K}f(t) \tag{2}$$

Where u_k is the modal component, ω_k is the central frequency for the modal component, $\delta(t)$ is the unit pulse function, and * is the convolution symbol.

In the VMD algorithm, the secondary penalty factor and the Lagrangian multiplication operator are used. Then, the alternating direction method is introduced. ${u_k}^{n+1}$, ${\omega_k}^{n+1}$, and ${\lambda}^{n+1}$ are constantly updated, so that the optimal solution of the variational constraint problem can be solved. The expression for the modal component ${u_k}^{n+1}$ is

$${u_k}^{n+1}=\underset{u_k\in X}{\operatorname{argmin}}\{\alpha\left\|a_t\{[(\delta(t)+\frac{j}{\pi t}]*u_k(t)\}e^{-j\omega_k t}\right\|_2^2+\left\|f(t)\ \sum_i u_i(t)+\frac{\lambda(t)}{2}\right\|_2^2\} \tag{3}$$

where α is the penalty factor, and λ is the Lagrange multiplier.

The expression for the modal component ${u_k}^{n+1}$ in frequency domain is

$$\hat{u}_k^{n+1}(\omega)=(\hat{f}(\omega)-\sum_i\hat{u}_i(\omega)+\frac{\hat{\lambda}(\omega)}{2})\frac{1}{1+2\alpha(\omega\ \ \omega_k)^2} \tag{4}$$

Where ω_k is the center of the modal component power spectrum. The Wiener filter is introduced, which makes the VMD algorithm have better noise robustness.

Similarly, the expression for the central frequency ${\omega_k}^{n+1}$ is

$$\omega_k^{n+1}(\omega)=\frac{\int_0^\infty\omega\left|\hat{u}_k(\omega)\right|^2d\omega}{\int_0^\infty\left|\hat{u}_k(\omega)\right|^2d\omega} \tag{5}$$

The stopping condition of the iteration is

$$\sum_{k=1}^{K}\left\|\hat{u}_k{}^{n+1}\ \ \hat{u}_k{}^{n}\right\|_2^2/\left\|\hat{u}_k{}^{n}\right\|_2^2<e \tag{6}$$

According to the previous derivation, we get the complete algorithm for VMD, summarized in algorithm 1.

Preprints (www.preprints.org) | NOT PEER-REVIEWED | Posted: 29 September 2017 doi:10.20944/preprints201709.0158.v1

algorithm 1: Complete optimization of VMD

Initialize $\{\hat{u}_k^1\},\{\hat{\omega}_k^1\},\{\hat{\lambda}^1\},n\leftarrow 0$

repeat

$n\leftarrow n+1$

for k = 1:K do

Update $\hat{u}_k^{n+1}$ **for all w >=0:**

$$\hat{u}_k^{n+1}(\omega)\leftarrow\frac{(\hat{f}(\omega)-\sum_i\hat{u}_i(\omega)+\frac{\hat{\lambda}(\omega)}{2})}{1+2\alpha(\omega-\omega_k)^2} \tag{7}$$

Update w_k:

$$\omega_k^{n+1}(\omega)\leftarrow\frac{\int_0^\infty\omega|\hat{u}_k(\omega)|^2d\omega}{\int_0^\infty|\hat{u}_k(\omega)|^2d\omega} \tag{8}$$

end for

Dual ascent for all w>=0:

$$\hat{\lambda}^{n+1}(\omega)\leftarrow\hat{\lambda}^n(\omega)+\beta[\hat{f}(\omega)-\sum_{k=1}^K\hat{u}_k^{n+1}(\omega)] \tag{9}$$

until convergence:

$$\sum_{k=1}^K\left\|\hat{u}_k^{n+1}-\hat{u}_k^n\right\|_2^2/\left\|\hat{u}_k^n\right\|_2^2<e \tag{10}$$

The VMD algorithm is a linear transformation, so the signal can be reconstructed. The reconstructed signal can be represented as:

$$\hat{f}(t)=\sum_{k=1}^K\hat{u}_k \tag{11}$$

Where $\hat{u}_k$ is the final modal component, after the iteration is stopped.

3. Euclidean distance

The vibration signals of vehicle structures are mostly symmetrical non Gauss signals. The PDF is calculated according to the Gauss curve stitching method based on empirical information, which is proposed by Steinwolf [27]. The PDF can fully reflect the statistical characteristics, the distribution law, the cumulant and the statistical moments of each order for non-Gauss signals. By comparing the ED between the PDF of the simulation signal and that of each BLIMF, the real BLIMFs can be selected to reconstruct the signal.

The PDF of the signal can be regarded as a point in the N dimensional space, and the ED between the point A and the point B can be represented as

$$ED=\sqrt{\sum_{n=1}^N(a_n-b_n)^2} \tag{12}$$

Preprints (www.preprints.org) | NOT PEER-REVIEWED | Posted: 29 September 2017 doi:10.20944/preprints201709.0158.v1

Where the coordinates of the point A are $(a_1, a_2, \ldots, a_n)$, and the coordinates of the point B are $(b_1, b_2, \ldots, b_n)$. The ED reflects the similarity of the two signals as the basis for signal reconstruction.

4. Proposed Method

Vibration signal analysis is usually used for condition monitoring and fault diagnosis. However, due to the complex structure of diesel engines, the vibration signals of diesel engines are usually multi-component, non-stationary and non-Gauss. In addition, there is a large amount of background noise in the vibration signals of diesel engines. Therefore, it is very difficult to extract fault characteristics from the vibration signals of diesel engines.

VMD is a recently proposed signal decomposition method, which is essentially composed of a number of adaptive Wiener filters, and has good noise robustness. Compared with the EMD method, the VMD method has a solid mathematical theoretical foundation, and can effectively alleviate or avoid a series of shortcomings in the EMD method. To verify the efficiency of the proposed method, several experiments on diesel engine connecting rod bearings faults are performed. The detailed experimental scheme is shown in Figure 1. Firstly, a signal channel vibration x(t), which is a wearing fault of the diesel engine connecting rod, is collected by the acceleration sensor vertically fixed on the diesel engine block. Secondly, the collected vibration signal x(t) is decomposed into six BLIMFs by VMD method. Thirdly, the PDFs of the collected vibration signal and each BLIMF are calculated respectively, and the ED between the PDF of the collected vibration signal and that of each BLIMF is calculated. Lastly, the relevant modes, which have smaller ED values, are thus selected to reconstruct the signal.

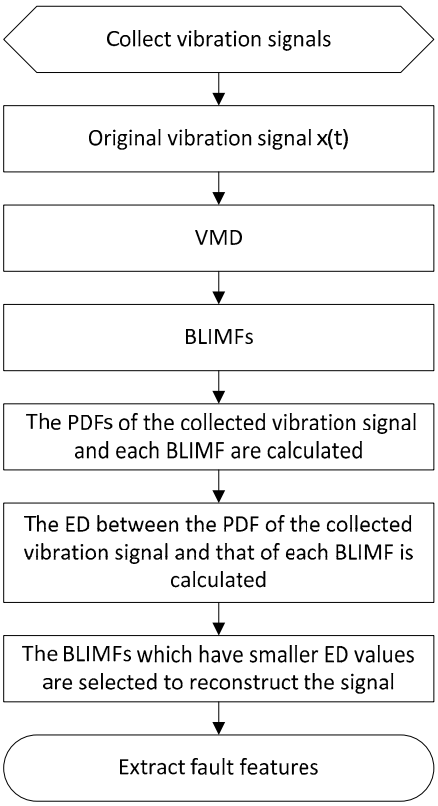

Figure 1. Detailed experimental scheme. BLIMF, band limited intrinsic mode functions; PDFs, probability density functions; ED, Euclidean distance.

Preprints (www.preprints.org) | NOT PEER-REVIEWED | Posted: 29 September 2017 doi:10.20944/preprints201709.0158.v1

5. Experimental Results

5.1. Simulation

Because of the complex structure of diesel engine, the number of vibration excitation source is large, and the vibration source signal is modulated by several components. Therefore, the established simulation signal must be multi-component and non-Gauss. According to document [28], the simulation signals are performed to verify the effectiveness of the proposed method, expressed in Equation (13-18). The mixed signal $S_{original}$ consists of three components, and the fault characteristic frequencies of the mixed signal are 50, 150 and 250 Hz. In addition, the mixed signal S_{noise} consists of four components, and the fourth component is the Gauss white noise.

$$s_1 = 1.6\cos(2\pi * 50t) * \sin(2\pi * 30t) \tag{13}$$

$$s_2 = \cos(2\pi * 150t) \tag{14}$$

$$s_3 = 0.8\cos(2\pi * 250t) \tag{15}$$

$$s_4 = randn(size(s_1)) \tag{16}$$

$$s_{\text{original}} = s_1 + s_2 + s_3 \tag{17}$$

$$s_{\text{noise}} = s_1 + s_2 + s_3 + s_4 \tag{18}$$

Where $S_{original}$ the original simulation signal before adding noise, and S_{noise} is the noisy simulation signal after adding noise. The waveforms of the four components are shown in Figure 2.

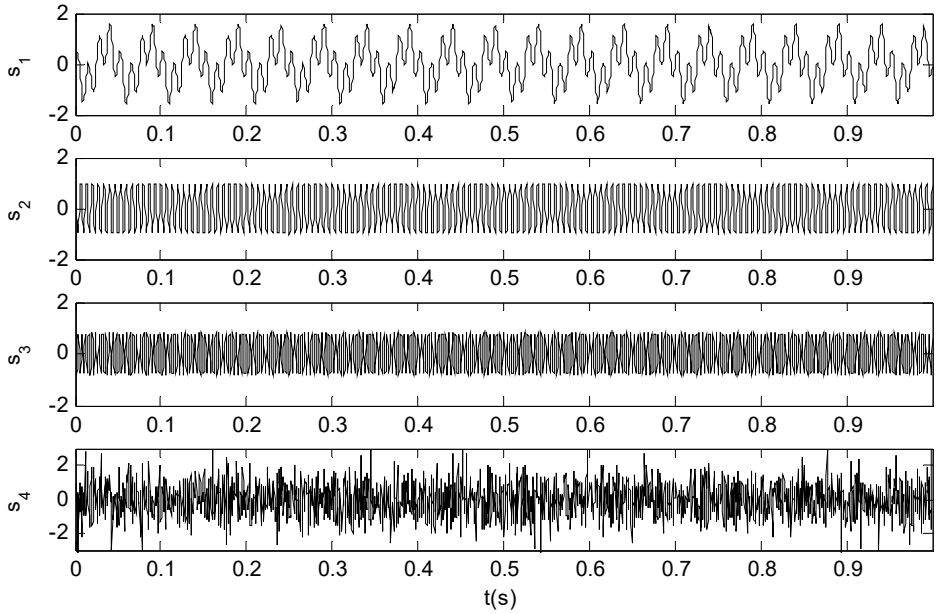

Figure 2. Source simulation signals.

The sampling frequency is 2048Hz, and the number of sampling points is 2048. The two mixed signals in the time domains are shown in Figure 3. As we can see from Figure 3, the shock component in the signal S_{noise} is weakened and the simulation signal becomes very cluttered, which is not convenient for fault feature extraction.

Preprints (www.preprints.org) | NOT PEER-REVIEWED | Posted: 29 September 2017 doi:10.20944/preprints201709.0158.v1

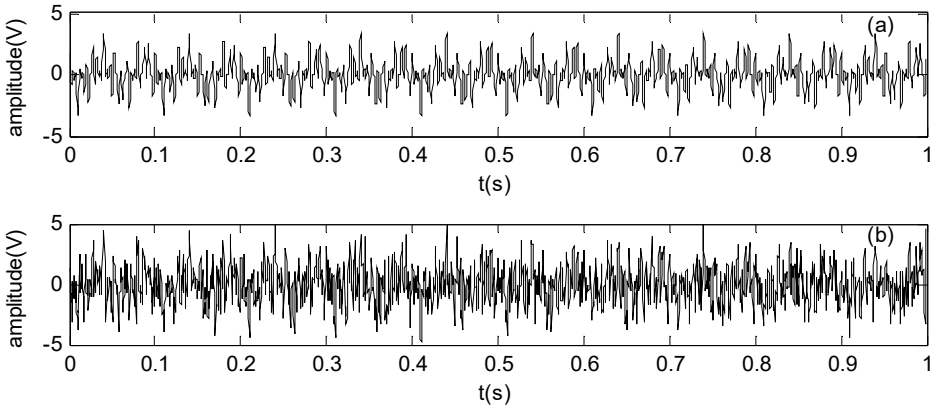

Figure 3. Simulation signals: (a) Waveform of the mixed signal $S_{original}$; (b) Waveform of the mixed signal S_{noise}.

Then, according to the detailed experimental scheme shown in Figure 1, the mixed signal S_{noise} is first decomposed into nine BLIMFs by the VMD method. The nine BLIMFs are shown in Figure 4.

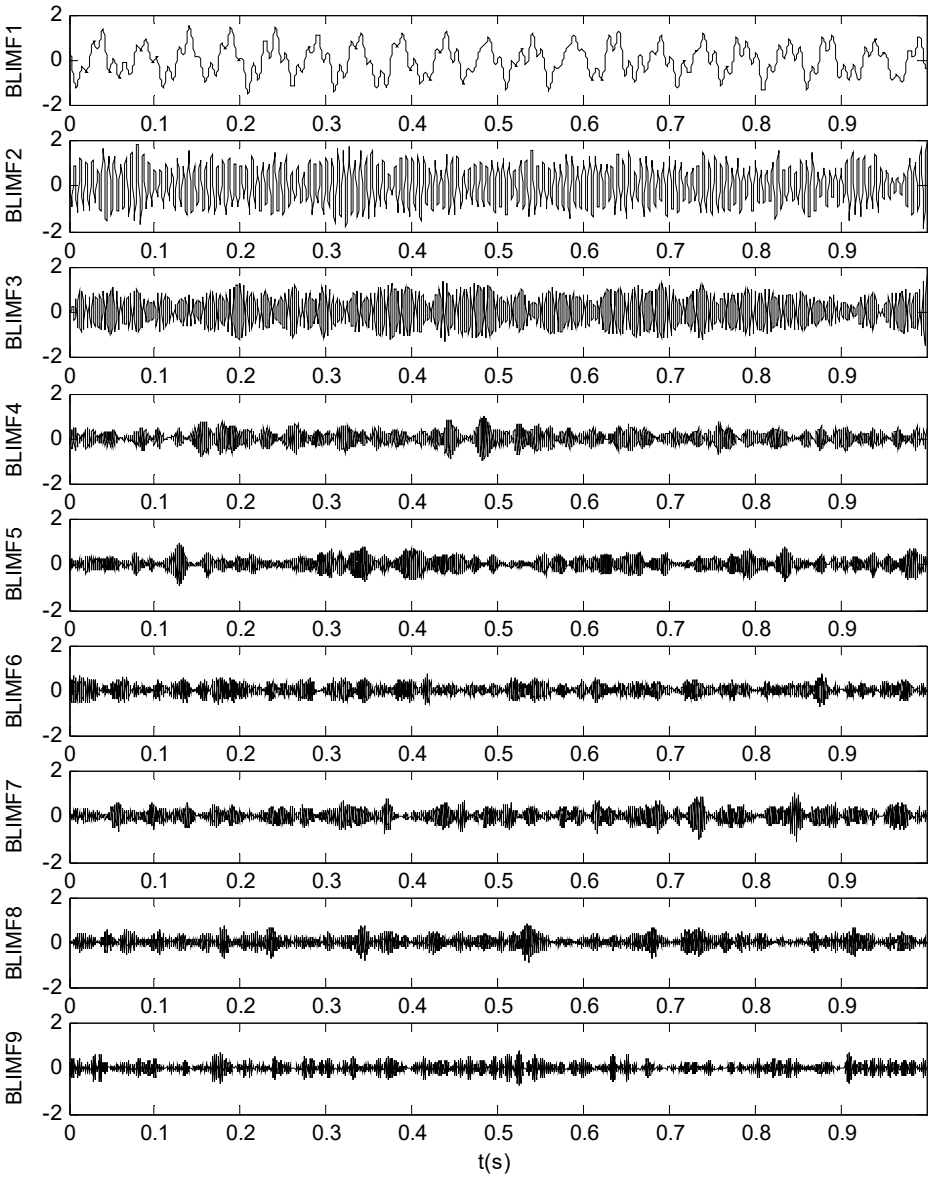

Figure 4. BLIMFs decomposed by the VMD method.

Preprints (www.preprints.org) | NOT PEER-REVIEWED | Posted: 29 September 2017 doi:10.20944/preprints201709.0158.v1

As we can see from Figure 4, pseudo component appears in the nine BLIMFs. Then the PDFs of the mixed signal S_{noise} and each BLIMF are calculated respectively. The PDFs are shown in Figure 5.

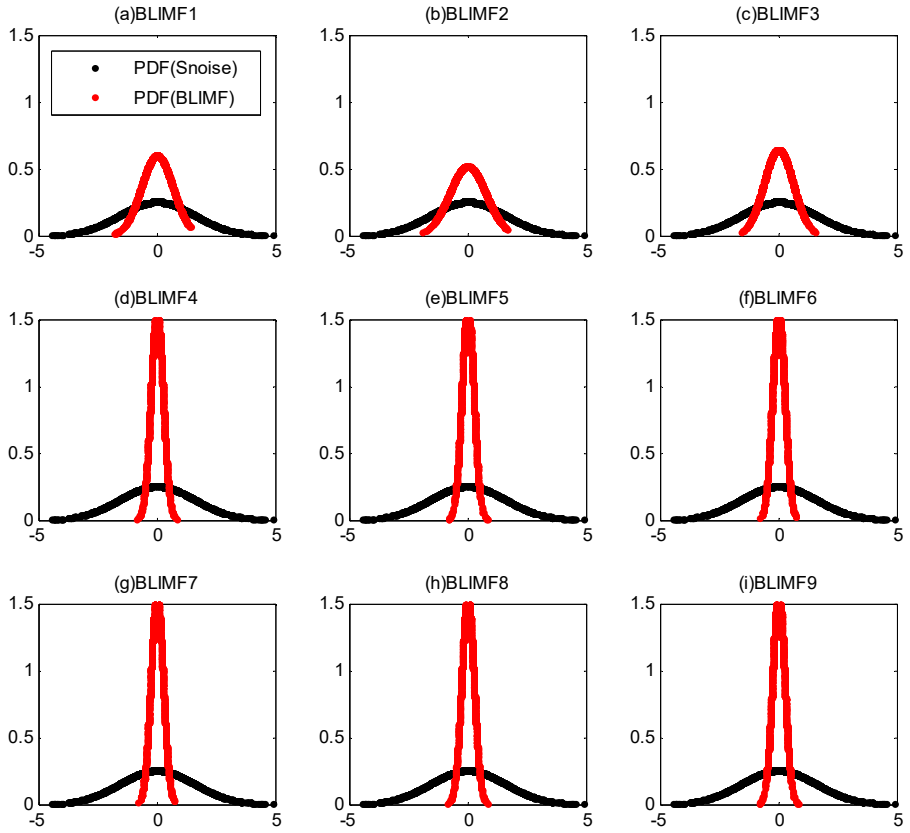

Figure 5. Superposition of the PDF of S_{noise} and those of its BLIMFs

As we can see from Figure 5, the PDFs of different BLIMF are not the same. In order to compare the differences among the BLIMFs more accurately, the Euclidean distance between the PDF of each BLIMF and that of the mixed signal S_{noise} is calculated respectively. Similarly, the Euclidean distance between the PDF of each IMF and that of the mixed signal S_{noise} is calculated by the EMD-ED method, and the correlation coefficient between each BLIMF and the mixed signal S_{noise} is calculated by the VMD-CORR method, as shown in Figure 6 and Table 1.

Table 1. Comparison of different methods.

VMD	Euclidean distance	EMD	Euclidean distance	VMD	correlation coefficient
BLIMF1	**11.63**	IMF1	**24.65**	BLIMF1	**0.60**
BLIMF2	**8.62**	IMF2	**12.19**	BLIMF2	**0.63**
BLIMF3	**13.68**	IMF3	**10.47**	BLIMF3	**0.45**
BLIMF4	92.37	IMF4	**16.15**	BLIMF4	**0.41**
BLIMF5	108.7	IMF5	**22.12**	BLIMF5	0.15
BLIMF6	111.4	IMF6	**25.87**	BLIMF6	0.14
BLIMF7	102.6	IMF7	86.37	BLIMF7	0.15
BLIMF8	97.58	IMF8	173.2	BLIMF8	0.15
BLIMF9	97.81	IMF9	313.4	BLIMF9	0.14

Preprints (www.preprints.org) | NOT PEER-REVIEWED | Posted: 29 September 2017 doi:10.20944/preprints201709.0158.v1

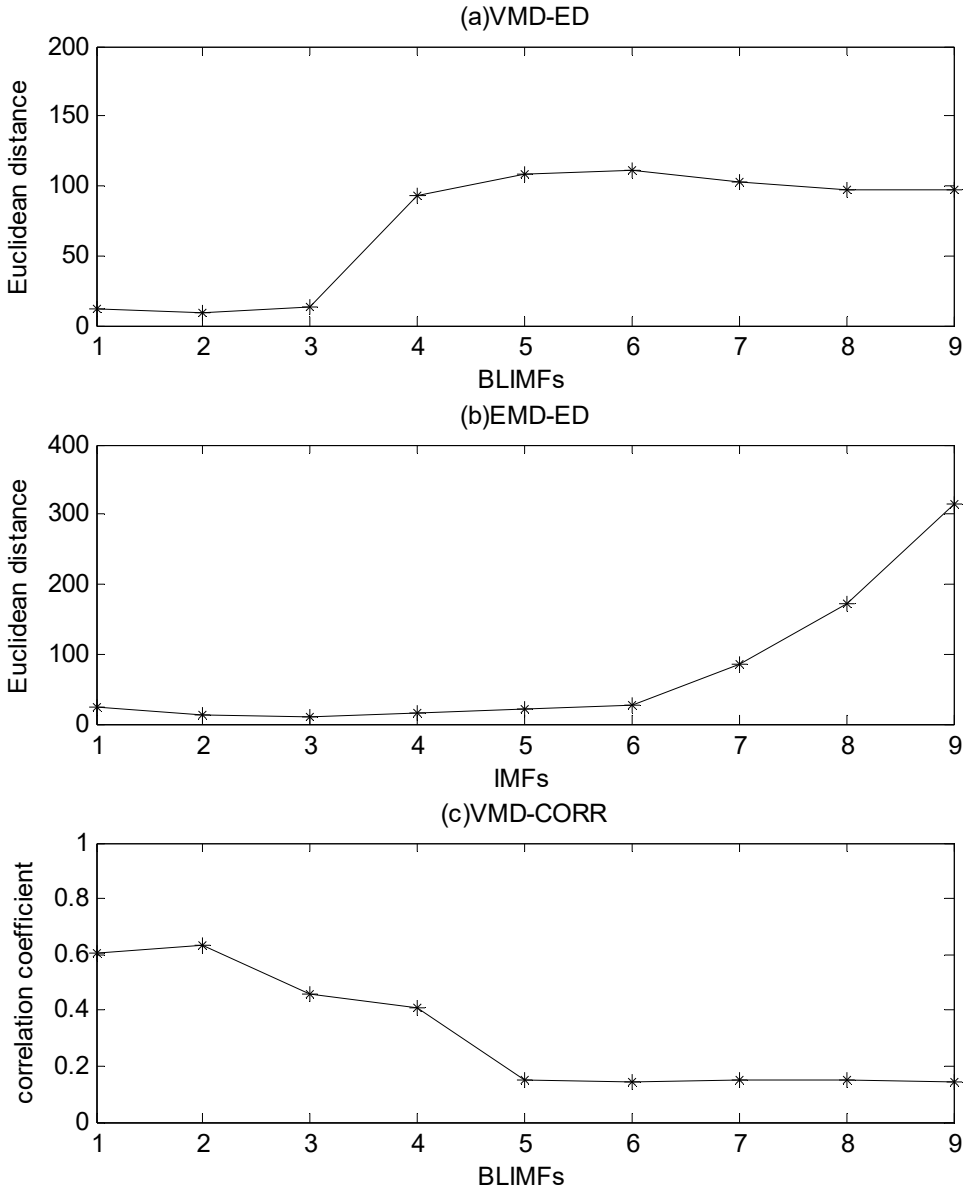

Figure 6. Comparison of different methods.

As can be seen from Figure 6 and Table 1, for the proposed method, the Euclidean distance of the first 3 BLIMFs is obviously smaller than that of other BLIMFs, which is consistent with the composition of the mixed signals. According to the experimental analysis, the Euclidean distance threshold is set to 20, and the BLIMFs with Euclidean distance less than 20 are used as the component of the reconstructed signal. Therefore, the first 3 BLIMFs are selected to reconstruct the signal to obtain the denoised signal. Similarly, using the EMD-ED and VMD-CORR methods mentioned above, the denoised signal is obtained. A part of the reconstructed signal is selected, and the reconstructed signals obtained by different methods are shown in figure 7.

Preprints (www.preprints.org) | NOT PEER-REVIEWED | Posted: 29 September 2017 doi:10.20944/preprints201709.0158.v1

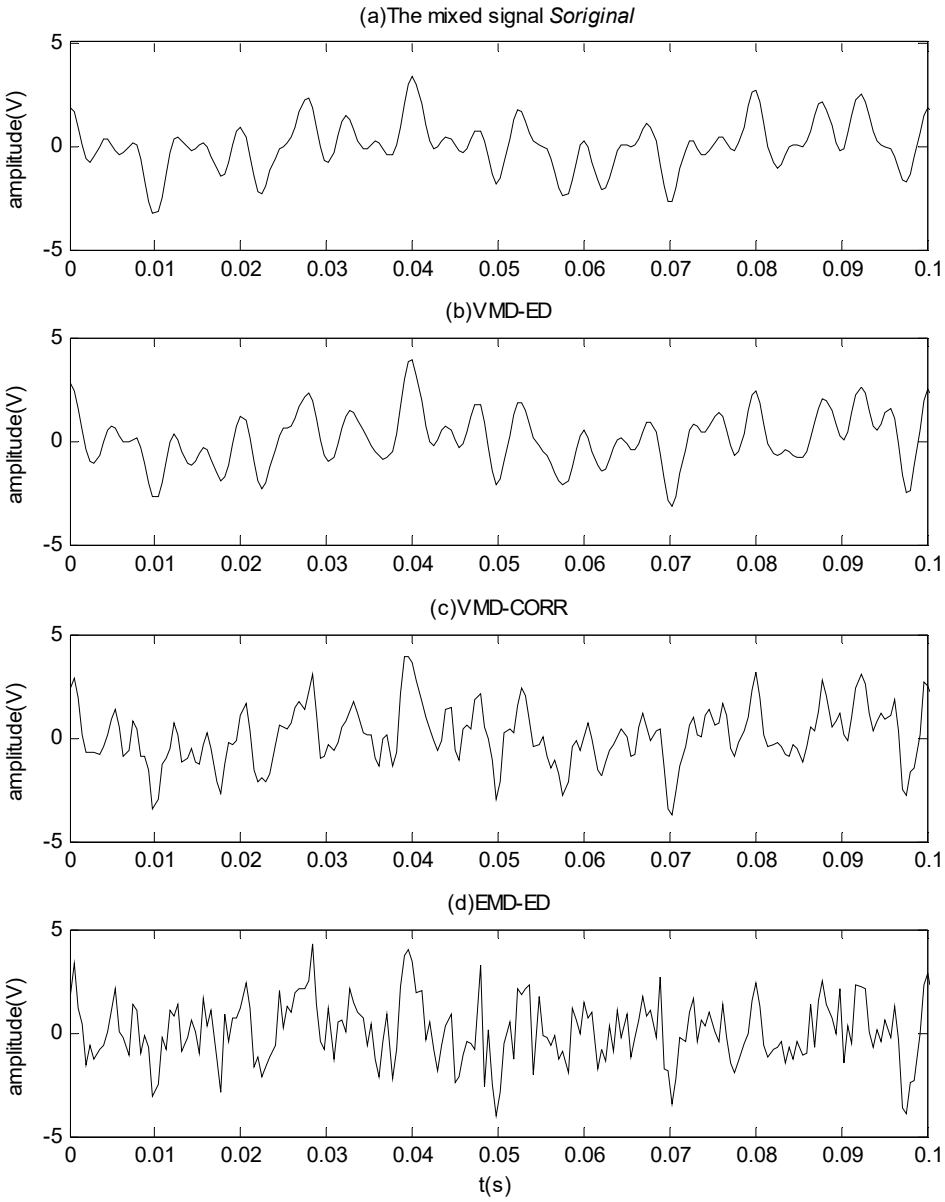

Figure 7. The reconstructed signals obtained by different methods.

As we can see from Figure 7, the reconstructed signal obtained by the proposed method is more similar to the mixed signal $S_{original}$. The noise in the signal is effectively removed, and the shock component is highlighted. Therefore, the method proposed in this paper is more effective in denoising. In the reconstructed signals obtained by EMD-ED and VMD-CORR, there are many spikes ,which are very different from the mixed signal $S_{original}$. Thus, the denoising effect of the two methods is not as good as the proposed method.

In order to evaluate the performance of different methods more comprehensively, different intensities of noise signals (-10 ~ 30dB) are added to the simulation signals. The signal to noise ratio (SNR), the root mean square error (RMSE) and the mean absolute error (MAE) of the reconstructed signals obtained by different methods are calculated respectively, as shown in Figure 8.

Preprints (www.preprints.org) | NOT PEER-REVIEWED | Posted: 29 September 2017 doi:10.20944/preprints201709.0158.v1

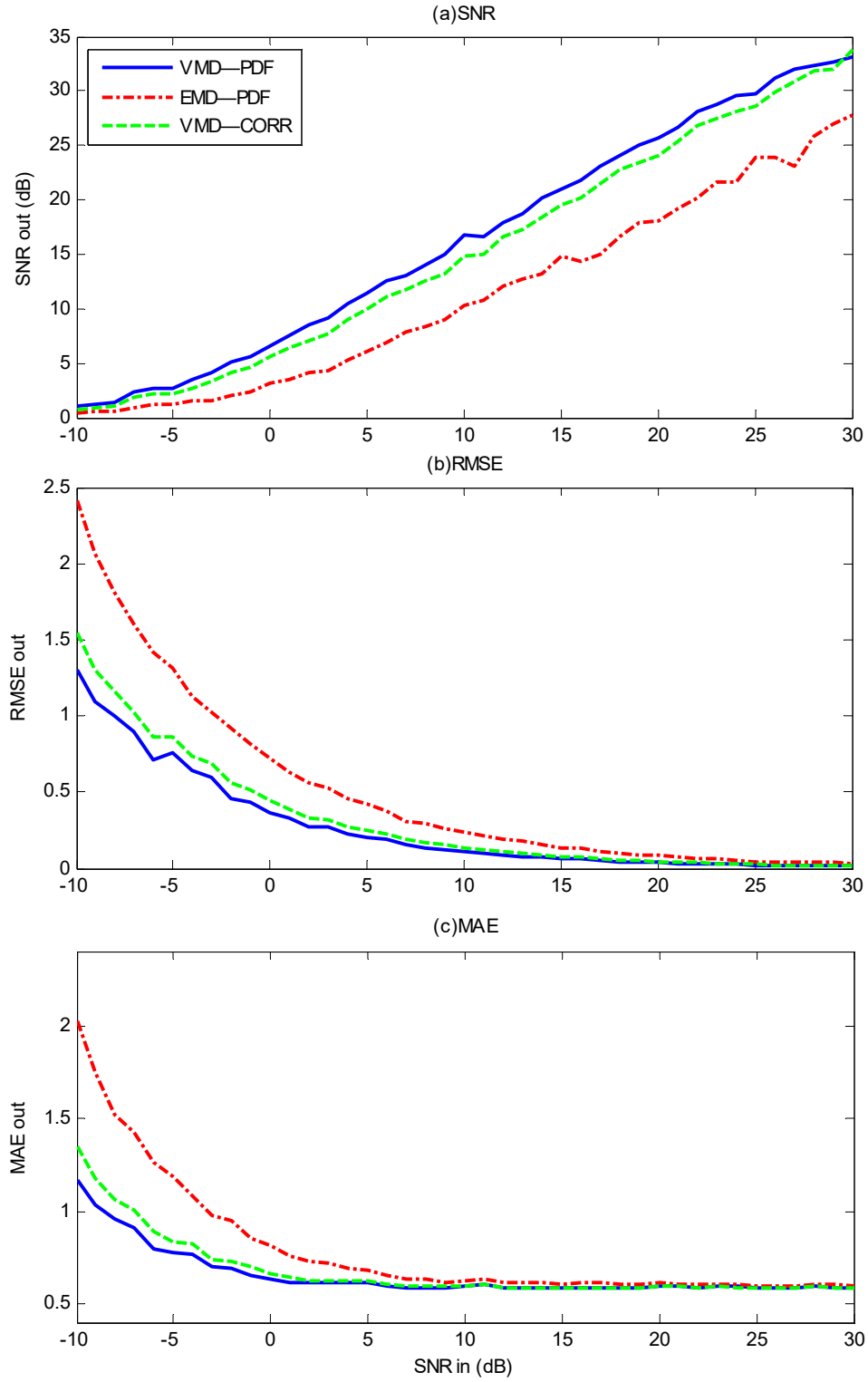

Figure 8. Comparison of denoising effects of different methods..

As we can see from Figure 8, the SNR of the proposed method is significantly higher than that of the other two methods, and RMSE and MAE are significantly lower than those of the other two methods. Therefore, the method proposed in this paper is better than other two methods in denoising.

Preprints (www.preprints.org) | NOT PEER-REVIEWED | Posted: 29 September 2017 doi:10.20944/preprints201709.0158.v1

5.2. Experiment Condition

The structure of diesel engine is complex and the working environment is abominable. As a result, it is prone to malfunction. The connecting rod bearing is located inside the engine, so it is difficult to diagnose the fault. In this paper, vibration signals are collected from the vibration sensors on the experimental stand, as shown in Figure 9. The basic parameters of the vibration sensor are shown in table 2. The engine on the experimental stand is Cummins 6BT diesel engine, and its parameters are shown in table 3.

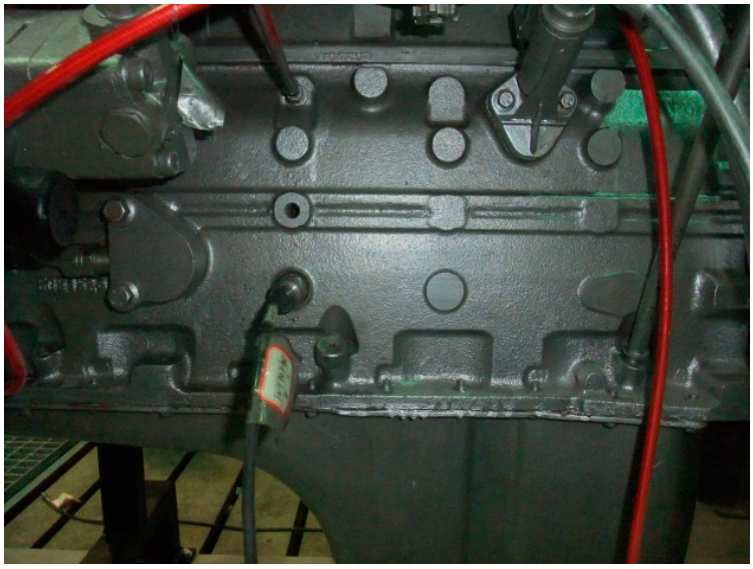

Figure 9. Measuring position of vibration sensor.

Table 3. Vibration sensor parameters

Model	Sensitivity	Frequency range (±3dB)	Range	Resolution	Temperature range	Weight	Output connector
603C01	100mV/g	0.5Hz–10KHz	±50g	350μg	-54-121℃	51 g	Top

Table 4. Basic parameters of the engine

Engine type	6BT5.9-G2	Fuel type	Diesel oil	Type	Inline 6 cylinders
Rated power (KW)	118	Compression ratio	17.5：1	Ignition sequence	153624
Rated speed (RPM)	2600	Continuous power (KW)	86	Maximum torque (N·m)	558
Radius (mm) ×Distance (mm)	102×120	Maximum torque speed (r/min)		1600	

The fourth connecting rod bearings of Cummins EQ6BT diesel engine are set with different clearance (0.10mm, 0.14mm, 0.20mm, 0.34mm) to simulate the normal, minor, moderate and severe wear of the connecting rod bearing. Vibration signals are collected on the left side of the fourth main bearings on the surface of the engine block. The sampling frequency is 20000Hz and the sampling points are 4096 points.

Preprints (www.preprints.org) | NOT PEER-REVIEWED | Posted: 29 September 2017 doi:10.20944/preprints201709.0158.v1

Testing temperature is important when acquiring vibration signals. In the experiment, the temperature of cooling water is measured to reflect the internal temperature of diesel engine. The temperature is controlled at 60-70 degrees C.

5.3. Data Acquired

The acquisition system is composed of collector, computer, sensor and connecting circuit, as shown in figure 10. The acquisition system set the speed of the engine to 1800r/min.

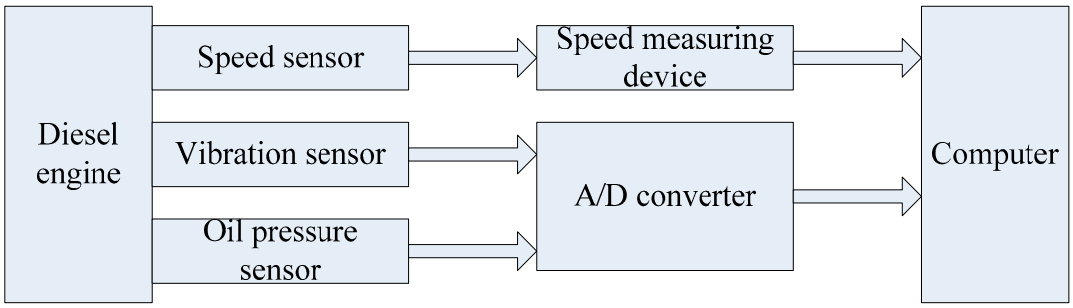

Figure 10. Vibration signal acquisition system.

The vibration signals of the engine under different wear conditions are collected, as shown in figure 11. In Figure 11, there is a large amount of background noise in the vibration signals of different wear conditions of the connecting rod, which is unfavorable to the extraction of fault features.

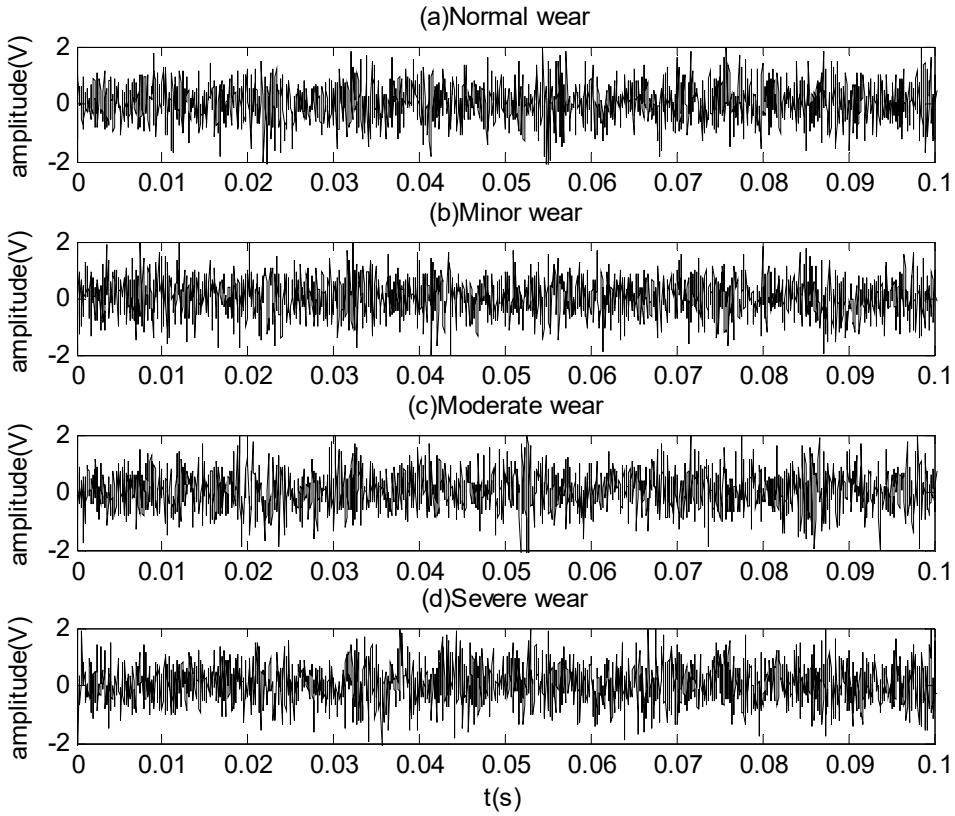

Figure 11. Vibration signals of connecting rod bearing under different wearing conditions.

Preprints (www.preprints.org) | NOT PEER-REVIEWED | Posted: 29 September 2017 doi:10.20944/preprints201709.0158.v1

5.4. Experimental Data Processing

The vibration signal of connecting rod bearing is analyzed according to the method proposed in this paper. The Euclidean distance between the PDF of each BLIMF and that of the vibration signals under different wear conditions is shown in Figure 12 and Table 5.

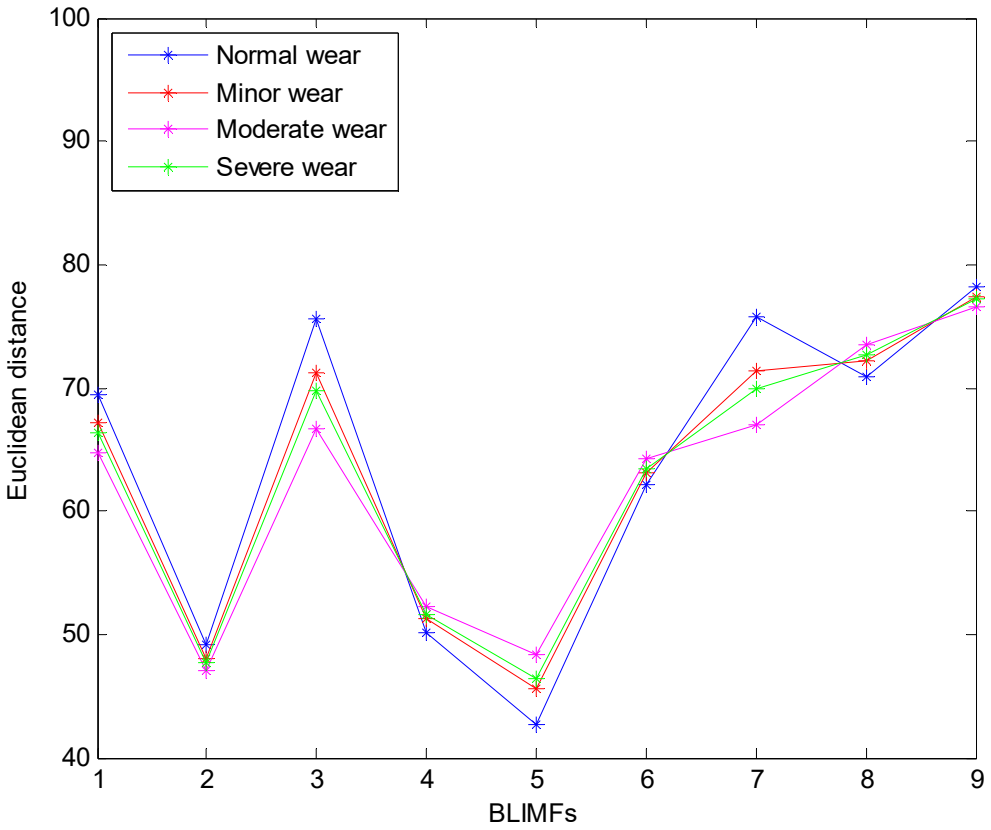

Figure 12. The Euclidean distance between the PDF of each BLIMF and that of the vibration signals under different wear conditions.

Table 5. The Euclidean distance between the PDF of each BLIMF and that of the vibration signals under different wear conditions.

BLIMFs	Normal wear	Minor wear	Moderate wear	Severe wear
BLIMF1	69.39	67.08	64.78	66.31
BLIMF2	**49.16**	**48.08**	**47.00**	**47.72**
BLIMF3	75.64	71.18	66.73	69.70
BLIMF4	**50.12**	**51.21**	**52.30**	**51.58**
BLIMF5	**42.62**	**45.51**	**48.40**	**46.47**
BLIMF6	62.06	63.13	64.20	63.48
BLIMF7	75.74	71.40	67.05	69.95
BLIMF8	70.82	72.17	73.52	72.62
BLIMF9	78.23	77.42	76.60	77.15

Preprints (www.preprints.org) | NOT PEER-REVIEWED | Posted: 29 September 2017 doi:10.20944/preprints201709.0158.v1

As we can see from Figure 12 and Table 5, the Euclidean distance of the BLIMF2, BLIMF4 and BLIMF5 is obviously smaller than that of other BLIMFs for the vibration signals under different wear conditions. According to the experimental analysis, the Euclidean distance threshold is set to 60, and the BLIMFs with Euclidean distance less than 60 are used as the component of the reconstructed signal. Therefore, the BLIMF1, BLIMF4 and BLIMF5 are selected to reconstruct the signal. A part of the reconstructed signal is selected, and the reconstructed signals under different wear conditions are shown in Figure 13.

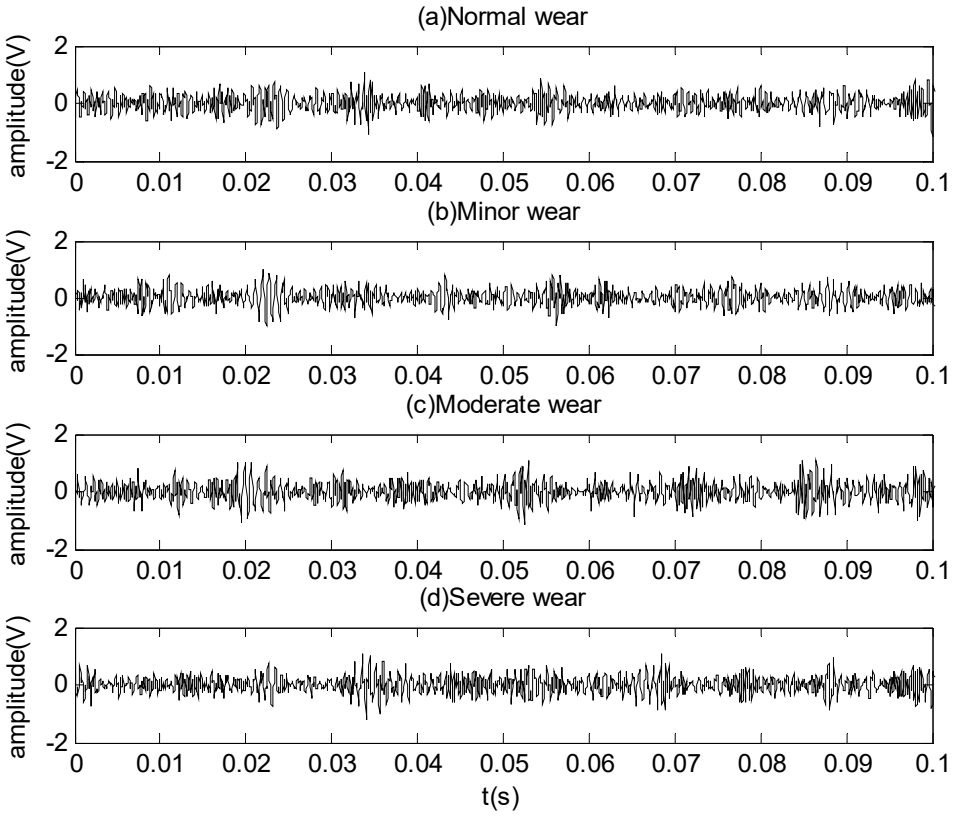

Figure 13. The reconstructed signals under different wear conditions.

As we can see from Figure 13, in the reconstructed signals under different wear conditions, the noise is reduced effectively. As compared with Figure 11, the signals become smoother and the shock components are more obvious. In order to further investigate the denoising effect of the proposed method, the vibration signals and reconstructed signals of different wear conditions are transformed by Morlet wavelet, as shown in Figure 14.

As we can see from Figure 14, compared with the vibration signals, the noise is effectively suppressed in the reconstructed signals, and the fault characteristics are obviously enhanced. Thus, the denoising method proposed in this paper is effective.

Preprints (www.preprints.org) | NOT PEER-REVIEWED | Posted: 29 September 2017 doi:10.20944/preprints201709.0158.v1

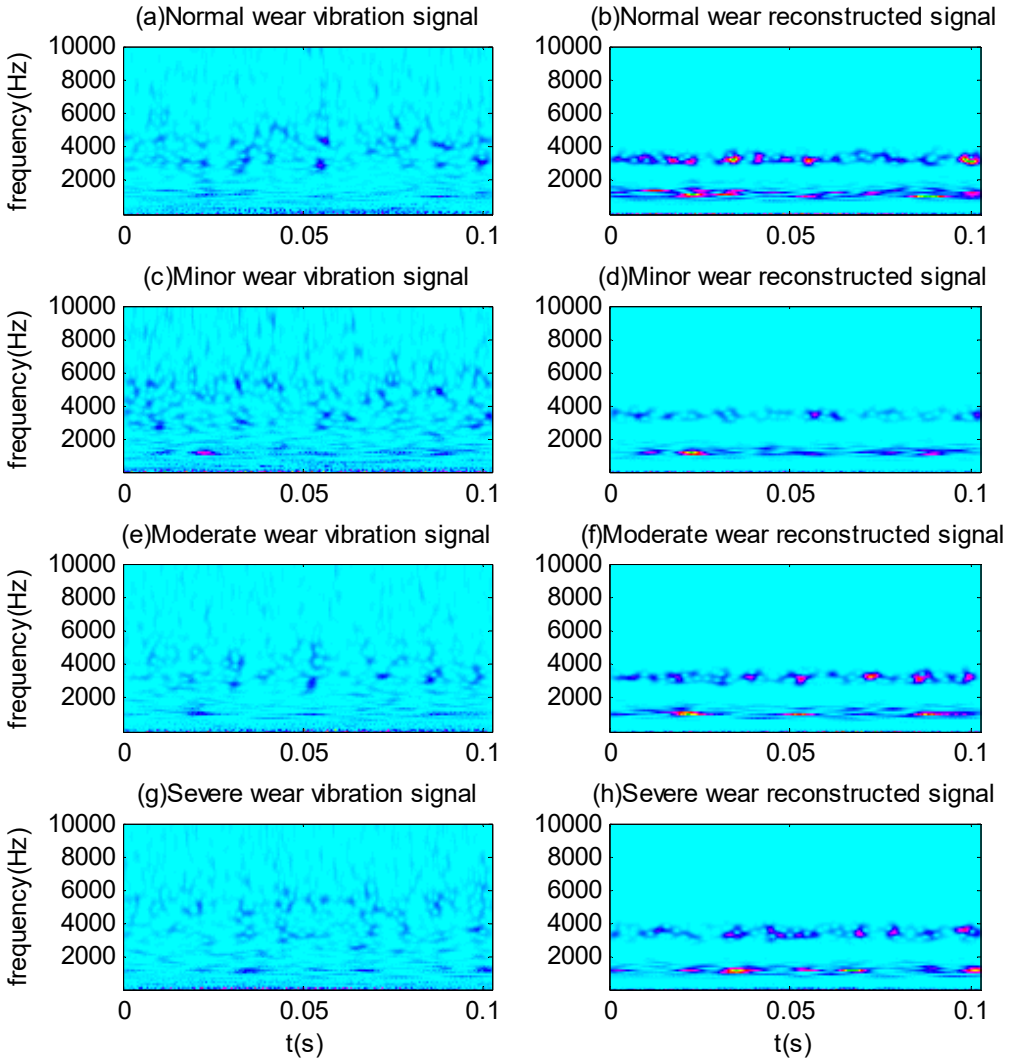

Figure 14. Time frequency analysis of vibration signals and reconstructed signals under different wear conditions

6. Conclusions

A new method based on VMD and Euclidean distance is proposed for diesel engine vibration signals, which usually contain a large amount of background noise. Firstly, the vibration signals are decomposed into several BLIMFs. Secondly, the PDFs of the vibration signals and each BLIMF are calculated respectively, and the Euclidean distance between the PDF of each BLIMF and that of the vibration signals is calculated. Finally, the BLIMFs with smaller Euclidean distance value are selected to reconstruct the signal. Compared with EMD-ED and VMD-CORR, the denoising method proposed in this paper is more effective. The proposed method is applied to the vibration signals of diesel engine connecting rod bearing wear faults. The noise is effectively suppressed, and the fault characteristics are obviously enhanced. However, the proposed method needs a given number of BLIMFs when vibration signal is decomposed by VMD, which is a drawback currently. Future work will focus on further optimization of the proposed method.

Acknowledgments: This work is partially supported by Key Project of the Army Equipment Department (Grant no.WG2015JJ010008).

Author Contributions: Gang Ren conceived of and designed the study. Jiajia Han and Xiangyu Jia were involved in the data collection and experimental work under the supervision of Gang Ren. Gang Ren wrote the paper under the supervision of Jide Jia. Jide Jia reviewed and edited the manuscript. All authors contributed to discussing and revising the manuscript.

Conflicts of Interest: The authors declare no conflicts of interest.

References

1. Chen, Y.; Zhang, P.; Wang, Z.; Yang, W.; Yang, Y. Denoising algorithm for mechanical vibration signal using quantum Hadamard transformation. Measurement. 2015, 66, 168-175.
2. Xie, Z.J.; Song B.Y.; Zhang Y.; Zhang F. Application of an Improved Wavelet Threshold Denoising Method for Vibration Signal Processing. Advanced Materials Research. 2014, 889-890:799-806.
3. Tang J.Y.; Chen W.T.; Chen S.Y.; Zhou W. Wavelet-based vibration signal denoising with a new adaptive thresholding function. Journal of Vibration & Shock.2009, 28 (7), 118-121.
4. Gao R. Study on Vibration Signal Denoising of Electric Spindle Based on Wavelet Transform. International Conference on Intelligent Human-machine Systems & Cybernetics, 2009, 1, 62-65.
5. Gao R. Analysis on Singularity of Fault Signals of High Spindle Based on Hermitian Wavelet. Journal of Computers.2011, 6 (4), 755-760.
6. To A. C.; Moore J. R.; Glaser S. D. Wavelet denoising techniques with applications to experimental geophysical data. Signal Processing.2009, 89(2), 144-160.
7. HUANG N. E.; SHEN Z.; LONG S. R. The empirical mode decomposition and the Hilbert spectrum fornonlinear and non-stationary time series analysis. Proceedings of the Royal Society. A. 1998, 454, 903-995.
8. HUANG N. E.; SHEN Z.; LONG S. R. A new view of non- linear water waves:The Hilbert spectrum. Annu. Rev. Fluid Mech. 1999, 31, 417-457.
9. Ai L.; Wang J.; Yao R. Classification of parkinsonian and essential tremor using empirical mode decomposition and support vector machine. Digital Signal Process.2011, 21(4), 543-550.
10. SU W.S.; Wang F.T.; Zhang Z.X.; Guo Z.G.; LI H.K. Application of EMD denoising and spectral kurtosis in early fault diagnosis of rolling element bearings. Journal of Vibration & Shock.2010, 22 (1), 3537-3540.
11. Lahmiri,; Boukadoum M. A weighted bio-signal denoising approach using empirical mode decomposition. Biomed. Eng. Lett.2015, 5(2), 131–139.
12. Huang C,; Wang H.; Long B. Signal Denoising Based on EMD. IEEE Circuits & Systems International Conference on Testing & Diagnosis.2009, 1-4.
13. Zhang Y.K.; Ma X.C.; Hua D.X.; Cui Y.A.; Sui L.S. An EMD-based denoising method for lidar signal. International Congress on Image & Signal Processing.2010, 8, 4016-4019.
14. Khaldi K.; Turki-Hadj Alouane M.; Boudraa A.O. A new EMD denoising approach dedicated to voiced speech signals. International Conference on Signals.2008, 1-5.
15. Kopsinis Y.; Mclaughlin S. Development of EMD-Based Denoising Methods Inspired by Wavelet

 doi:10.20944/preprints201709.0158.v1

Thresholding. IEEE Transactions on Signal Processing.2009, 57 (4), 1351-1362.

16. Yang G.; Liu Y.; Wang Y.; Zhu Z. EMD interval thresholding denoising based on similarity measure to select relevant modes. Signal Processing.2015, 109 (C), 95-109.
17. Komaty A.; Boudraa A.; Dare D. Emd-based filtering using the Hausdorff distance. IEEE International Symposium on Signal Processing and Information Technology.2012, pp. 000292–000297.
18. Dragomiretskiy K.; Zosso D. Variational Mode Decomposition. IEEE Transactions on Signal Processing.2013, 62(3), 531-544.
19. Zhao C.; Feng Z. P. Application of multi-domain sparse features for fault identification of planetary gearbox. Measurement.2017, 104, 169-179.
20. An X. L.; Tang Y. J. Denoising of hydropower unit vibration signal based on variational mode decomposition and approximate entropy. Transactions of the Institute of Measurement and Control. 2016, 38(3), 282-292.
21. Li Z. P.; Chen J. L.; Zi Y. Y. Independence-oriented VMD to identify fault feature for wheel set bearing fault diagnosis of high speed locomotive. Mechanical Systems and Signal Processing. 2017, 85, 512-529.
22. E J. W.; Bao Y. L.; Ye J. M. Crude oil price analysis and forecasting based on variational mode decomposition and independent component analysis. Physica A.2017, 484, 412-427.
23. An X. L.; Tang Y. J. Application of variational mode decomposition energy distribution to bearing fault diagnosis in a wind turbine. Transactions of the Institute of Measurement and Control. 2017, 39(7), 1000-1006.
24. Liu Y. Y.; Yang G. L.; Li M. Variational mode decomposition denoising combined the detrended fluctuation analysis. Signal Processing.2016, 125, 349-364.
25. Yao J. C.; Xiang Y.; Qian S. C. Noise source identi- fication of diesel engine based on variational mode decomposition and robust independent component analysis. Applied Acoustics. 2017, 116, 184-194.
26. Zhang M.; Jiang Z. N.; Feng K. Research on variational mode decomposition in rolling bearings fault diagnosis of the multistage centrifugal pump. Mechanical Systems and Signal Processing. 2017, 93, 460-493.
27. Steinwolf A. Approximation and simulation of probability distributions with a variable kurtosis value. Computational Statistics & Data Analysis.1996, 21(2), 163-180.